The Canadian Mineralogist
Vol. 36, pp. 1253-1265 (1998)

THE ROLE OF Ti IN HYDROGEN-DEFICIENT AMPHIBOLES: SODIC–CALCIC AND SODIC AMPHIBOLES FROM COYOTE PEAK, CALIFORNIA

FRANK C. HAWTHORNE[1], ROBERTA OBERTI AND ALBERTO ZANETTI

CNR Centro di Studio per la Cristallochimica e la Cristallografia, via Ferrata 1, I–27100 Pavia, Italy

GERALD K. CZAMANSKE

750 West Greenwich Place, Palo Alto, California 94303, U.S.A.

ABSTRACT

The crystal structures of eleven sodic–calcic and sodic amphiboles from lithic-wacke inclusions in the alkali ultramafic diatreme at Coyote Peak, Humboldt County, California, have been refined to *R* values of 1–2% using single-crystal Mo*K*α X-ray data. The crystals used in the collection of the intensity data were subsequently analyzed by electron- and ion-microprobe techniques. They were analyzed for H and Li, and the unit formulae were calculated on the basis of 24(O,OH,F). Site populations were assigned from the results of site-scattering refinement and stereochemical analysis, taking into account the unit formula determined for each crystal. These amphiboles range in composition from fluororichterite and fluorian eckermannite through titanian fluorian potassic-richterite, titanian fluorian richterite and titanian fluororichterite to titanian oxygenian arfvedsonite; Ti contents range from 0.12 to 0.75 *apfu*, and (OH + F) contents range from 2.00 to 0.84 *apfu*. Where Ti ≤ 0.13 *apfu*, (OH + F) ≈ 2.0 *apfu*. Where Ti > 0.13 *apfu*, Ti varies linearly with the amount of O^{2-} at the O(3) site [= 2 – (OH + F)], with a slope of 0.52. Thus Ti is incorporated into these amphiboles *via* the substitution $Ti^{4+} + 2\ O^{2-} \rightarrow (Mg,Fe^{2+}) + 2\ (OH)^-$. Variation in *M*(1)–O(3), *M*(3)–O(3) and *M*(1)–*M*(1) distances as a function of Ti content of the amphibole indicates that all Ti in excess of 0.13 *apfu* occurs at the *M*(1) site, where it is associated with a short *M*(1)–O(3) distance; Ti up to 0.13 *apfu* occurs at the *M*(2) site. The presence of O^{2-} at the O(3) site in these amphiboles induces a range of values of both the O(5)–O(6)–O(7) angle, and the difference between the *M*(4)–O(5) and *M*(4)–O(6) bond-lengths not found in normal [O(3) = OH,F] amphiboles. Some features of the formula derived from electron-microprobe results can be used as diagnostic indicators of the presence of extensive $^{[6]}Li$ and O^{2-} substitutions in monoclinic amphiboles.

Keywords: amphibole, crystal-structure refinement, electron-microprobe analysis, secondary-ion mass spectrometry, hydrogen, titanium, Coyote Peak, California.

SOMMAIRE

Les structures cristallines de onze amphiboles sodi-calciques et sodiques d'enclaves lithiques incluses dans le diatrème ultramafique alcalin de Coyote Peak, comté de Humboldt, en Californie, ont été affinées sur monocristaux, jusqu'à des valeurs résiduelles de R égales à 1–2%, en utilisant le rayonnement Mo*K*α. Les cristaux utilisés pour les affinements ont ensuite été analysés par microsondes électronique et ionique. L'hydrogène et le lithium ont été dosés, et les formules structurales calculées sur la base de 24 (O, OH, F). L'occupation des sites a été déterminée à partir des résultats de mesures de densités électroniques, et des analyses stéréochimiques, en prenant en considération la formule unitaire déterminée pour chaque cristal. Les compositions de ces amphiboles peuvent être décrites comme des solutions solides impliquant la fluororichtérite, l'eckermannite fluorée, pour les pôles dépourvus de titane, et la potassic-richtérite et la richtérite titanifères fluorées, la fluororichtérite titanifère et l'arfvedsonite titanifère oxygénée. Les teneurs en titane sont comprises entre 0.12 et 0.75 atomes par unité formulaire (*apuf*), et les teneurs en (OH + F) vont de 2.00 à 0.84 *apuf*. Pour Ti < 0.13 *apuf*, la somme (OH + F) est égale à 2.0 *apuf*. Pour Ti > 0.13 *apuf*, la teneur en O^{2-} au site O(3) [= 2 – (OH +F)] varie linéairement avec le contenu en Ti, avec une pente de 0.52. On en déduit que l'incorporation de Ti dans la structure de l'amphibole se fait selon le mécanisme $Ti^{4+} + 2O^{2-} \rightarrow (Mg,Fe^{2+}) + 2(OH)^-$. Les variations des distances *M*(1)–O(3), *M*(3)–O(3) et *M*(1)–*M*(1) avec la teneur en titane de l'amphibole montrent que tout le titane en quantité supérieure à 0.13 *apuf* est situé au site *M*(1), où il génère des distances *M*(1)–O(3) particulièrement courtes. Jusqu'à une teneur en Ti < 0.13 *apuf*, le titane est situé au site *M*(2). La présence de O^{2-} au site O(3) dans ces amphiboles induit un domaine

[1] Presently may be accessed at the Department of Geological Sciences, University of Manitoba, Winnipeg, Manitoba R3T 2N2. *E-mail address*: frank_hawthorne@umanitoba.ca

de variation des angles O(5)–O(6)–O(7) et une différence entre longueurs de liaisons *M*(4)–O(5) et *M*(4)–O(6) inconnus dans les amphiboles normales, ayant O(3) = (OH + F). Certaines caractéristiques de la formule telle que dérivée à partir des données de microsonde électronique sont diagnostiques de la présence de quantités importantes de $^{[6]}Li$ et O^{2-} dans une amphibole monoclinique.

(Traduit par la Rédaction)

Mots-clés: amphiboles, affinement de structure, microsonde électronique, spectrométrie de masse des ions secondaires, hydrogène, titane, Coyote Peak, Californie.

Introduction

Titanium is an important minor component in many amphiboles, yet its behavior is still not completely understood. Evidence from spectroscopic (Waychunas 1987, Otten & Buseck 1987), crystallographic (Oberti *et al.* 1992) and crystal-chemical (Della Ventura *et al.* 1991) analyses has established that Ti is in the tetravalent state in amphiboles. Della Ventura *et al.* (1991) and Oberti *et al.* (1992) showed that Ti^{4+} may occur in tetrahedral coordination in potassic-richterite and potassic-fluororichterite, in which it occupies the *T*(2) site. In other amphiboles, Ti^{4+} has been assigned to the tetrahedral sites where calculation of the unit formula shows (Si + Al) < 8.00 atoms per formula unit, *apfu* (*e.g.*, Czamanske & Dillet 1988, Czamanske & Atkin 1985), but there is no direct proof for this particular occupancy. Moreover, Oberti *et al.* (1992) argued that $^{[4]}Ti^{4+}$ should be restricted to potassic-richterite and potassic-fluororichterite. The behavior of Ti^{4+} in octahedral coordination is less clear. Kitamura *et al.* (1975) showed by neutron diffraction that Ti is strongly ordered at the *M*(1) site in oxygenian kaersutite. Unpublished X-ray structure-refinements of oxygenian kaersutite samples (Cannillo *et al.* 1988) show a split *M*(1') position shifted toward O(3), suggesting that Ti^{4+} at *M*(1) is displaced toward the adjacent O(3) sites in order to satisfy the bond-valence requirements of O^{2-} at the O(3) site. Similar behavior was observed in some crystals of potassic-fluororichterite by Oberti *et al.* (1992), but they suggested that not all of the $^{[6]}Ti^{4+}$ is involved in this type of behavior. Thus, although there are good indications as to the behavior of $^{[6]}Ti^{4+}$ in amphiboles, the general problem is still not resolved.

Czamanske & Atkin (1985) examined chemical variations in zoned sodic–calcic and sodic amphiboles from lithic-wacke fragments which reacted after being caught up in the alkali ultramafic diatreme at Coyote Peak, Humboldt County, California. These amphiboles contain up to 0.76 Ti^{4+} *apfu* (~6.5 wt% TiO_2), with a fairly continuous compositional variation over this range. The more Ti-rich compositions have (Si + Al) < 8.00 *apfu*, such that Czamanske & Atkin (1985) assigned up to 0.20 Ti *apfu* to the tetrahedral sites. Citing Charles (1977), Czamanske & Atkin (1985) suggested that the richteritic cores of these Coyote Peak amphiboles crystallized at quite low values of $f(O_2)$ (*i.e.*, 10^{-21} at 600°C and 0.1 GPa on the QFM buffer), and the more Ti-rich arfvedsonitic rims, at even lower $f(O_2)$ values. Such conditions contrast strongly with those expected for kaersutite and oxygenian kaersutite on which considerable work has been done, suggesting that characterization of the Coyote Peak amphiboles might contribute further to our understanding of Ti in amphiboles.

Petrological Setting and Sample Selection

An alkaline ultramafic diatreme (260 × 500 m at surface) penetrates a lithic-wacke sandstone sequence of the Franciscan assemblage, 20 km southeast of Orick, California. A brief discussion of the petrography, origin and evolution of the igneous rocks of this occurrence were presented by Morgan *et al.* (1985). Czamanske & Atkin (1985) described the remarkable history of metasomatism and crystal growth recorded in lithic-wacke fragments that were caught up in, and reacted with, their ultramafic host magma. Small fragments of wacke were totally recrystallized, whereas larger fragments display strong rim-to-core zonation. Observation of abundant microcline, aegirine and sodic amphibole in fully reacted wacke, as compared to abundant albite, quartz and clay in unreacted wacke, led Czamanske & Atkin (1985) to postulate that the reaction process involved loss of Si from the wacke fragments, and mass influx of K (bulk fragments may contain up to 12 wt% K_2O). Sodium released from albite (1) combined first with Ti and Fe to form myriads of strongly zoned Ti-rich aegirine crystals, (2) promoted formation of larger strongly zoned Ti-rich inclusion-free grains of sodic amphibole, and (3) ultimately was bound in a late-stage zeolite similar to natrolite. The sequence of crystallization and the zonation of the pyroxenes and amphiboles were ascribed to decreasing $f(O_2)$ and temperature, as the oxidized sedimentary assemblage reacted with the rapidly cooling reduced ultramafic melt.

Fragments of amphibole grains were extracted by hand from crushed samples of the most intensely reacted wacke fragments. The sample codes and names (IMA-approved nomenclature, Leake *et al.* 1997) of the amphibole crystals used in this work are listed in Table 1, sorted in order of increasing Ti-content. Additional characterization of samples CYP 52 and CYP 101

is presented in Czamanske & Atkin (1985), whereas samples CYP 132, 177 and 300 were specifically chosen for this study by GKC.

Analytical Methods

X-ray data collection and structure refinement

Experimental details are as described by Oberti *et al.* (1992). Unit-cell parameters, *R* indices and other information pertinent to data collection and refinement are given in Table 2. Selected interatomic distances and angles are listed in Table 3, and the refined site-scattering powers are listed in Table 4. Final atomic coordinates and anisotropic-displacement parameters may be obtained from The Depository of Unpublished Data, CISTI, National Research Council, Ottawa, Ontario K1A 0S2.

Electron- and ion-microprobe analyses

The crystals used in the collection of the X-ray intensity data were subsequently mounted, polished and analyzed by electron- and ion-microprobe techniques. Electron-microprobe analysis was done following the procedures described by Oberti *et al.* (1992). Ion-microprobe analysis for Li and H was done according to the procedures described by Ottolini *et al.* (1993, 1995). The estimated accuracy for H is ~10%.

Calculation of the formula unit

As the H and F contents of these amphiboles were measured, the unit formulae were calculated on the basis of 24(O,OH,F). As shown below, the presence of O^{2-} at O(3) is balanced by the presence of Ti^{4+} at *M*(1), and hence there is no reason for Fe^{3+} to occur at the *M*(1) or *M*(3) sites [*i.e.*, Fe^{3+} is restricted to the *M*(2) site]. The Fe^{3+} content of *M*(2) was derived from the observed <*M*(2)–O> distance and the mean bond-length – aggregate-cation-radius relation of Hawthorne (1983a), and the final unit formulae were calculated using the resultant Fe^{3+}/Fe^{2+} values. The chemical compositions and resulting unit formulae (in *apfu*) are given in Table 5.

TABLE 1. COYOTE PEAK AMPHIBOLES: SAMPLE NUMBERS, TiO_2 CONTENT AND NAMES

Sample	SEQ*	TiO_2 (wt%)	Name
CYP 177	763	1.10	Fluororichterite
CYP 300	740	1.76	Fluorian richterite
CYP 177	760	1.86	Fluorian eckermannite
CYP 177	764	1.95	Fluorian richterite
CYP 177	765	2.06	Fluorian richterite
CYP 300	739	2.19	Fluorian richterite
CYP 132	758	2.54	Titanian fluorian potassic-richterite
CYP 52	741	3.30	Titanian fluorian richterite
CYP 101	749	3.97	Titanian fluororichterite
CYP 101	750	5.69	Titanian fluorian richterite
CYP 52	745	6.51	Titanian oxygenian arfvedsonite

* SEQ: sequence number in amphibole database at Pavia.

Site Populations

The site populations were assigned on the basis of (1) the refined site-scattering values (Table 4), (2) the unit formulae derived from the chemical compositions determined by electron- and ion-microprobe analyses (Table 5), and (3) the observed bond-lengths (Table 3). The results are given in Table 6.

The T(1) and T(2) sites

The unit formulae (Table 5) indicate that these amphiboles contain small amounts (< 0.30 *apfu*) of tetrahedrally coordinated Al. In most amphiboles, $^{[4]}$Al is ordered at the *T*(1) site, although in high-temperature (~1000°C) amphiboles, disorder of $^{[4]}$Al over the *T*(1) and *T*(2) sites does occur (Oberti *et al.* 1995a). As $^{[4]}$Al (r = 0.39 Å) is larger than $^{[4]}$Si (r = 0.26 Å, Shannon 1976), the ordering behavior of $^{[4]}$Al should be reflected in the variation in mean bond-lengths at the *T*(1) and *T*(2) sites. The variation in <*T*(1)–O> as a function of Al (Fig. 1) is linear and agrees with the relation proposed by Oberti *et al.* (1995a). This linearity indicates

TABLE 2. CRYSTAL DATA AND STRUCTURE REFINEMENT INFORMATION FOR COYOTE PEAK AMPHIBOLES

	763	740	760	764	765	739	758	741	749	750	745
a (Å)	9.903	9.913	9.894	9.900	9.913	9.906	9.997	9.882	9.893	9.899	9.845
b (Å)	18.004	18.043	17.991	18.002	18.017	18.049	18.059	18.028	18.064	18.090	18.018
c (Å)	5.275	5.291	5.289	5.286	5.281	5.288	5.302	5.283	5.282	5.289	5.296
β (°)	104.35	104.29	104.02	104.12	104.34	104.39	104.43	104.17	104.30	104.25	103.86
V (Å^3)	911.0	917.1	913.5	913.7	913.8	915.8	926.9	912.5	914.7	918.0	912.1
Sp. Gr.	*C2/m*	*C2/m*	*C2/m*	*C2/m*	*C2/m*	*C2/m*	*C2/m*	*C2/m*	*C2/m*	*C2/m*	*C2/m*
No. $\|F\|$	1379	1391	1386	1382	1387	1391	1405	1385	1388	1393	1383
No. $\|F_o\|$	1024	890	1041	1090	965	983	1142	902	881	763	774
R(obs) %	1.7	1.4	1.5	1.5	1.8	1.6	1.9	1.7	1.8	1.7	1.7
R(all) %	3.0	3.5	2.6	2.4	3.2	3.0	2.6	3.6	3.9	4.8	4.7

* Standard deviations in the last digit: $a \le 4$; $b \le 8$; $c \le 3$; $\beta \le 3$

TABLE 3. SELECTED INTERATOMIC DISTANCES (Å)* AND ANGLES (°)* FOR COYOTE PEAK AMPHIBOLES

		763	740	760	764	765	739	758	741	749	750	745
T(1)–O(1)		1.601	1.609	1.604	1.601	1.603	1.612	1.605	1.602	1.606	1.607	1.607
T(1)–O(5)		1.628	1.633	1.626	1.628	1.628	1.633	1.631	1.625	1.627	1.623	1.623
T(1)–O(6)		1.628	1.632	1.623	1.625	1.625	1.635	1.626	1.625	1.626	1.622	1.623
T(1)–O(7)		1.637	1.640	1.637	1.637	1.637	1.640	1.637	1.634	1.635	1.635	1.631
<*T*(1)–O>		1.623	1.628	1.622	1.623	1.623	1.630	1.625	1.622	1.623	1.622	1.621
T(2)–O(2)		1.612	1.612	1.612	1.611	1.611	1.615	1.615	1.614	1.611	1.615	1.616
T(2)–O(4)		1.580	1.583	1.585	1.581	1.583	1.583	1.587	1.582	1.581	1.582	1.583
T(2)–O(5)		1.666	1.665	1.665	1.665	1.665	1.664	1.669	1.664	1.665	1.668	1.661
T(2)–O(6)		1.679	1.679	1.676	1.678	1.680	1.677	1.682	1.676	1.678	1.683	1.671
<*T*(2)–O>		1.634	1.635	1.635	1.634	1.635	1.635	1.638	1.634	1.634	1.637	1.633
M(1)–O(1)	x2	2.066	2.072	2.071	2.071	2.069	2.067	2.081	2.069	2.068	2.069	2.070
M(1)–O(2)	x2	2.051	2.071	2.064	2.063	2.060	2.070	2.074	2.073	2.077	2.089	2.093
M(1)–O(3)	x2	2.067	2.080	2.071	2.072	2.065	2.070	2.092	2.040	2.033	2.024	2.021
<*M*(1)–O>		2.062	2.074	2.069	2.069	2.065	2.069	2.082	2.061	2.059	2.061	2.062
M(2)–O(1)	x2	2.193	2.192	2.195	2.199	2.198	2.190	2.189	2.206	2.208	2.210	2.190
M(2)–O(2)	x2	2.086	2.092	2.077	2.084	2.091	2.093	2.100	2.091	2.105	2.109	2.086
M(2)–O(4)	x2	1.992	1.991	1.966	1.977	1.988	1.999	1.980	1.987	1.997	1.999	1.963
<*M*(2)–O>		2.090	2.092	2.079	2.087	2.092	2.094	2.090	2.095	2.103	2.106	2.080
M(3)–O(1)	x4	2.070	2.081	2.088	2.084	2.074	2.077	2.100	2.084	2.084	2.097	2.115
M(3)–O(3)	x2	2.040	2.052	2.057	2.053	2.046	2.051	2.069	2.049	2.050	2.056	2.082
<*M*(3)–O>		2.050	2.072	2.078	2.074	2.065	2.068	2.090	2.072	2.073	2.083	2.104
M(4)–O(2)	x2	2.418	2.415	2.420	2.419	2.416	2.413	2.427	2.412	2.415	2.412	2.417
M(4)–O(4)	x2	2.365	2.357	2.372	2.370	2.364	2.351	2.389	2.364	2.362	2.365	2.376
M(4)–O(5)	x2	2.871	2.875	2.913	2.903	2.884	2.863	2.888	2.909	2.904	2.927	2.953
M(4)–O(6)	x2	2.581	2.587	2.570	2.574	2.586	2.586	2.597	2.573	2.580	2.577	2.539
<*M*(4)–O>		2.559	2.558	2.569	2.566	2.562	2.553	2.575	2.565	2.565	2.570	2.572

that all Al is [4]-coordinated and is completely ordered at the *T*(1) site, confirming the results of the renormalization procedure used to produce the unit formulae.

There is also a small variation in the <*T*(2)–O> values, from 1.633 to 1.638 Å. Oberti *et al.* (1995a) have shown that variations of this magnitude in <*T*(2)–O> can be due to changes in next-nearest-neighbor site-populations with no change in the *T*(2) site-populations. Is this the case for the Coyote Peak amphiboles, or is there Ti^{4+} at the *T*(2) site? The presence of Ti^{4+} at *T*(2) would cause anomalously low displacement values at *T*(2) during the refinement if the scattering from *T*(2) were modeled as Si only. The displacement values at *T*(2) are normal, indicating that there is no $^{[4]}Ti$ in the Coyote Peak amphiboles.

The behavior of Ti^{4+}

Where Ti^{4+} is in octahedral coordination, its behavior is not well characterized in amphiboles. Small high-valence [6]-coordinated cations tend to order at the *M*(2) site, and on the basis of this general observation, the small amounts of $^{[6]}Ti$ usually present in most amphiboles are assigned to the *M*(2) site (Hawthorne 1983a). However, there has been no direct proof for this assignment. In kaersutite and oxygenian kaersutite, Ti^{4+} tends to be strongly (but not completely) ordered at the *M*(1) site (Kitamura *et al.* 1975, Pechar *et al.* 1989). In richterite, Oberti *et al.* (1992) showed that $^{[6]}Ti^{4+}$ is very strongly ordered at the *M*(1) site, with small amounts at *M*(2) or *M*(3), or both. Furthermore, Oberti *et al.* (1992) proposed that Ti^{4+} enters the *M*(1) site *via* the substitution

$$^{M(1)}Ti^{4+} + 2\ ^{O(3)}O^{2-} \rightarrow {}^{M(1)}(Mg,Fe^{2+}) + 2\ ^{O(3)}OH^{-} \quad (1)$$

and suggested that Ti^{4+} at *M*(1) is locally associated with O^{2-} at the two adjacent O(3) sites.

The Coyote Peak amphiboles provide an excellent test for the above proposal, as both OH (as H_2O) and F

Table 3. cont.

		763	740	760	764	765	739	758	741	749	750	745
A–O(5)	x4	2.886	2.894	2.854	2.864	2.885	2.905	2.901	2.863	2.874	2.865	2.820
A–O(6)	x4	3.150	3.163	3.187	3.177	3.160	3.152	3.177	3.174	3.167	3.181	3.210
A–O(7)	x2	2.492	2.495	2.511	2.509	2.502	2.485	2.579	2.492	2.488	2.495	2.513
<*A*–O>		2.918	2.922	2.918	2.918	2.919	2.920	2.947	2.913	2.914	2.918	2.915
A(*m*)–O(5)	x2	3.023	3.047	2.999	3.015	3.028	3.064	3.016	3.027	3.026	3.033	3.021
A(*m*)–O(5)	x2	2.848	2.857	2.812	2.821	2.844	2.869	2.856	2.816	2.831	2.820	2.775
A(*m*)–O(6)	x2	2.775	2.757	2.801	2.786	2.777	2.738	2.854	2.768	2.774	2.770	2.750
A(*m*)–O(7)		2.500	2.512	2.520	2.524	2.514	2.507	2.588	2.518	2.504	2.519	2.547
A(*m*)–O(7)		3.168	3.147	3.168	3.155	3.158	3.132	3.253	3.127	3.142	3.119	3.056
A(*m*)–O(7)		2.600	2.614	2.622	2.619	2.610	2.607	2.650	2.605	2.602	2.613	2.658
<*A*(*m*)–O>		2.840	2.844	2.837	2.838	2.842	2.843	2.883	2.830	2.834	2.833	2.817
A(2)–O(5)	x2	2.355	2.508	2.528	2.492	2.354	2.670	2.487	2.449	2.524	2.409	2.523
A(2)–O(6)	x2	2.729	2.853	2.924	2.878	2.739	2.961	2.843	2.843	2.884	2.815	2.969
A(2)–O(7)	x2	2.589	2.544	2.546	2.554	2.599	2.503	2.635	2.549	2.528	2.565	2.541
<*A*(2)–O>		2.558	2.635	2.666	2.642	2.564	2.711	2.655	2.614	2.646	2.596	2.678
T(1)–O(5)–*T*(2)		136.0	135.9	135.9	135.9	136.2	136.2	136.2	136.3	136.5	136.9	136.5
T(1)–O(6)–*T*(2)		136.5	137.1	137.6	137.2	136.9	136.8	137.2	137.1	136.7	136.7	137.7
T(1)–O(7)–*T*(1)		137.6	138.2	139.3	138.9	138.0	137.8	140.4	138.6	138.2	138.6	141.0
O(6)–O(5)–O(7)		110.5	110.2	112.5	112.0	111.0	109.6	111.7	112.0	111.4	112.2	114.5
T(1)–*T*(2)–*T*(1)		118.9	119.1	119.4	119.2	119.0	118.9	119.3	119.2	119.1	119.1	119.8
T(2)–*T*(1)–*T*(1)		90.5	90.4	90.1	90.3	90.5	90.5	90.3	90.3	90.4	90.4	89.9

* Standard devations are ≤ 2 in the final digit

TABLE 4. REFINED SITE-SCATTERING VALUES (*epfu*) AND CORRESPONDING VALUES CALCULATED FROM THE UNIT FORMULAE DERIVED FROM MICROPROBE ANALYSIS (MP) FOR COYOTE PEAK AMPHIBOLES

	763	740	760	764	765	739	758	741	749	750	745
M(1)	27.2	30.7	30.8	30.2	29.2	30.4	37.2	33.1	34.4	39.4	43.4
M(2)	31.9	36.4	39.1	36.8	33.4	35.3	40.5	36.0	37.3	39.6	43.2
M(3)	12.8	15.5	15.0	14.9	14.2	15.0	17.0	15.6	16.4	18.4	18.4
Σ*M*(1,2,3)	71.9	82.7	84.9	82.0	76.8	80.7	94.7	84.7	88.1	97.4	105.0
Σ*M*(1,2,3)^{MP}	69.5	81.4	85.7	82.4	76.9	82.2	94.0	83.0	86.4	96.6	106.4
M(4)	29.6	30.0	25.6	27.0	29.7	31.6	27.3	28.3	29.8	29.6	23.6
M(4)^{MP}	30.1	29.4	25.6	27.1	29.6	30.4	27.3	28.5	29.7	28.9	23.3
A	14.0	13.5	13.9	14.0	13.9	13.2	16.2	13.4	13.3	13.4	13.7
A^{MP}	12.7	13.0	13.3	13.5	13.4	12.6	16.2	12.9	12.5	12.8	13.4
O(3)	17.2	16.9	16.0	16.9	17.1	17.1	16.6	17.0	17.1	17.1	16.8
O(3)^{MP}	17.3	16.8	16.7	16.7	17.0	16.8	16.5	16.9	17.0	16.6	16.3

* Standard deviations are ≤1 in the final digit for XREF data.

TABLE 5. CHEMICAL COMPOSITIONS AND UNIT FORMULAE* OF COYOTE PEAK AMPHIBOLES

	763	740	760	764	765	739	758	741	749	750	745
SiO_2	56.32	52.71	55.29	55.00	54.73	53.02	51.82	54.78	53.93	52.87	52.47
Al_2O_3	0.29	1.41	0.21	0.25	0.45	1.74	0.94	0.26	0.38	0.23	0.09
TiO_2	1.10	1.76	1.86	1.95	2.06	2.19	2.54	3.30	3.97	5.69	6.51
Fe_2O_3	0.00	0.00	3.77	1.74	0.00	0.19	2.22	0.18	0.00	0.00	4.54
FeO	4.99	12.25	10.52	10.33	8.73	11.45	15.50	11.18	12.70	17.06	18.43
MnO	0.12	0.28	0.25	0.23	0.20	0.26	0.43	0.14	0.26	0.33	0.15
MgO	20.26	15.21	14.02	15.46	17.52	15.65	10.78	14.91	13.73	9.78	5.74
CaO	5.98	5.33	2.56	3.65	5.44	5.97	3.65	4.66	5.44	4.76	0.90
Na_2O	6.10	6.28	7.74	7.30	6.21	5.94	6.00	6.82	6.35	6.51	8.70
K_2O	1.87	1.73	2.00	1.93	2.03	1.68	3.43	1.62	1.48	1.50	1.51
Li_2O	0.02	0.00	0.05	0.02	0.02	0.00	0.06	0.01	0.01	0.02	0.17
F	2.82	1.58	1.43	1.58	2.09	1.82	1.06	1.95	2.16	1.20	0.51
H_2O	0.79	1.19	1.21	1.19	0.99	0.98	1.17	0.65	0.47	0.46	0.58
O=F	−1.19	−0.67	−0.60	−0.67	−0.88	−0.77	−0.45	−0.82	−0.91	−0.51	−0.21
Total	99.47	99.06	100.31	99.96	99.59	100.12	99.15	99.64	99.97	99.90	100.09
Si	7.954	7.762	8.002	7.954	7.878	7.706	7.846	7.978	7.905	7.947	7.993
Al	0.046	0.238	0.000	0.043	0.076	0.294	0.154	0.022	0.066	0.041	0.007
ΣT	8.000	8.000	8.002	7.997	7.954	8.000	8.000	8.000	7.971	7.988	8.000
Al	0.002	0.007	0.036	–	–	0.004	0.014	0.023	–	–	0.009
Fe^{3+}	–	–	0.411	0.189	–	0.021	0.253	0.020	–	–	0.520
Fe^{2+}	0.589	1.509	1.273	1.249	1.051	1.392	1.963	1.361	1.557	2.144	2.348
Mn	0.014	0.035	0.031	0.028	0.024	0.032	0.055	0.017	0.032	0.042	0.019
Ti	0.117	0.195	0.202	0.212	0.223	0.239	0.289	0.361	0.438	0.643	0.746
Mg	4.266	3.339	3.025	3.333	3.760	3.391	2.433	3.237	3.000	2.191	1.303
Li	0.011	–	0.029	0.012	0.012	–	0.036	0.006	0.006	0.012	0.104
ΣC	4.999	5.085	5.007	5.023	5.070	5.079	5.043	5.026	5.033	5.032	5.049
Ca	0.905	0.825	0.397	0.567	0.839	0.930	0.592	0.727	0.854	0.767	0.147
Na	1.095	1.175	1.603	1.433	1.161	1.070	1.408	1.273	1.146	1.233	1.853
ΣB	2.000	2.000	2.000	2.000	2.000	2.000	2.000	2.000	2.000	2.000	2.000
Na	0.575	0.618	0.569	0.614	0.572	0.604	0.353	0.653	0.659	0.664	0.716
K	0.337	0.325	0.369	0.356	0.373	0.312	0.663	0.301	0.277	0.288	0.293
ΣA	0.912	0.943	0.938	0.970	0.945	0.916	1.016	0.954	0.936	0.952	1.009
OH	0.744	1.169	1.168	1.148	0.951	0.950	1.182	0.631	0.460	0.461	0.589
F	1.260	0.736	0.655	0.723	0.951	0.837	0.508	0.898	1.001	0.570	0.246
Σ	2.004	1.905	1.823	1.871	1.902	1.787	1.690	1.529	1.461	1.031	0.835
O	0.000	0.095	0.177	0.129	0.098	0.213	0.310	0.471	0.539	0.969	1.163

* see text for discussion of normalization procedure

contents of the amphiboles have been measured directly for the single crystals on which the diffraction experiments were done. Figure 2 shows the variation in Ti^{4+} content of the amphiboles as a function of the O^{2-} content (= 2 – OH – F *apfu*) of the O(3) site. For zero content of O^{2-} at O(3), the Ti^{4+} content of the amphibole is approximately 0.13 *apfu*. Above ~0.13 Ti^{4+} *apfu*, there is a linear correlation between Ti^{4+} and O^{2-} at O(3), with a correlation coefficient $R = 0.99$, a slope of 0.52, and an intercept of 0.13 Ti^{4+} at zero O^{2-} content of O(3). This indicates that below a $^{[6]}Ti^{4+}$ content of 0.13 *apfu*, Ti^{4+} substitutes into these amphiboles by one (as yet unspecified) mechanism, whereas above a $^{[6]}Ti^{4+}$ content of 0.13 *apfu*, Ti^{4+} substitutes into these amphiboles according to the relation $Ti^{4+} + 2\ O^{2-} \rightarrow (Mg,Fe^{2+}) + 2\ OH^-$. Note that this relation, unlike relation (1), is not site-specific. Local bond-valence arguments indicate that such a substitutional relation should involve a cation site immediately adjacent to O(3), limiting it to $M(1)$ and $M(3)$, but additional evidence is needed to make the relation more site-specific.

A very straightforward way to examine the environment of the O(3) site is to look at the variation in $M(1)$–O(3) and $M(3)$–O(3) as a function of Ti^{4+} content. In most amphiboles, the $M(1)$ and $M(3)$ sites are dominated by Mg ($^{[6]}r = 0.72$ Å) and Fe^{2+} ($^{[6]}r = 0.78$ Å) [except for Mg-rich pargasite, in which $M(3)$ can contain considerable Al (Oberti *et al.* 1995b), and kaersutite]. Incorporation of Ti^{4+} ($^{[6]}r = 0.605$ Å) at the $M(1)$ or $M(3)$ sites will produce a general shortening of both $M(1)$–O and $M(3)$–O distances; this shortening is expected to be large for the $M(1)$–O(3) and $M(3)$–O(3) bonds if Ti^{4+} substitutes and is locally associated with O^{2-} at the adjacent O(3) sites. There is a strong contraction in $M(1)$–O(3) with increasing Ti^{4+} in the amphibole (Fig. 3a), whereas there is an increase in $M(3)$–O(3) with increasing Ti^{4+} (Fig. 3b). The values of $M(1)$–O(3) and $M(3)$–O(3) are also affected by variations in the Fe^{2+}

TABLE 6. SITE POPULATIONS (*apfu*) FOR COYOTE PEAK AMPHIBOLES

		763	740	760	764	765	739	758	741	749	750	745
T(1)	Al	0.05	0.24	0.04	0.04	0.08	0.30	0.17	0.06	0.07	0.04	0.01
	Si	3.95	3.76	3.96	3.96	3.92	3.70	3.83	3.94	3.93	3.96	3.99
T(2)	Si	4.00	4.00	4.00	4.00	4.00	4.00	4.00	4.00	4.00	4.00	4.00
M(1)	Mg	1.77	1.50	1.49	1.53	1.60	1.51	1.01	1.28	1.17	0.75	0.44
	Fe	0.23	0.44	0.44	0.39	0.31	0.38	0.83	0.49	0.52	0.74	0.96
	Ti	–	0.06	0.08	0.08	0.09	0.11	0.16	0.23	0.31	0.51	0.60
M(2)	Ti	0.12	0.13	0.13	0.13	0.13	0.13	0.13	0.13	0.13	0.13	0.13
	Fe^{3+}	–	0.21	0.49	0.22	0.05	0.20	0.36	0.14	0.03	0.07	0.72
	Fe^{2+}	0.48	0.58	0.50	0.60	0.53	0.51	0.73	0.62	0.83	0.95	0.56
	Mg	1.40	1.08	0.88	1.05	1.29	1.16	0.78	1.11	1.01	0.85	0.59
M(3)	Mg	0.93	0.75	0.74	0.79	0.84	0.79	0.58	0.73	0.69	0.54	0.36
	Fe^{2+}	0.06	0.25	0.23	0.20	0.15	0.21	0.38	0.26	0.30	0.45	0.53
	Li	0.01	–	0.03	0.01	0.01	–	0.04	0.01	0.01	0.01	0.11
M(4)	Ca	0.90	0.82	0.40	0.57	0.84	0.93	0.59	0.73	0.85	0.77	0.15
	Na	1.10	1.18	1.60	1.43	1.16	1.07	1.41	1.27	1.15	1.23	1.85
A	Na	0.58	0.62	0.57	0.61	0.57	0.60	0.34	0.65	0.66	0.66	0.71
	K	0.34	0.33	0.37	0.36	0.37	0.31	0.66	0.30	0.28	0.29	0.29
	Σ	0.92	0.95	0.94	0.97	0.94	0.91	1.00	0.95	0.94	0.95	1.00
O(3)	OH	0.74	1.16	1.18	1.13	0.91	0.95	1.18	0.64	0.42	0.44	0.56
	F	1.26	0.72	0.66	0.71	0.91	0.84	0.50	0.90	0.96	0.54	0.24
	Σ	2.00	1.88	1.84	1.84	1.82	1.78	1.68	1.54	1.38	0.98	0.80
	O	–	0.12	0.16	0.16	0.18	0.22	0.32	0.46	0.62	1.02	1.20

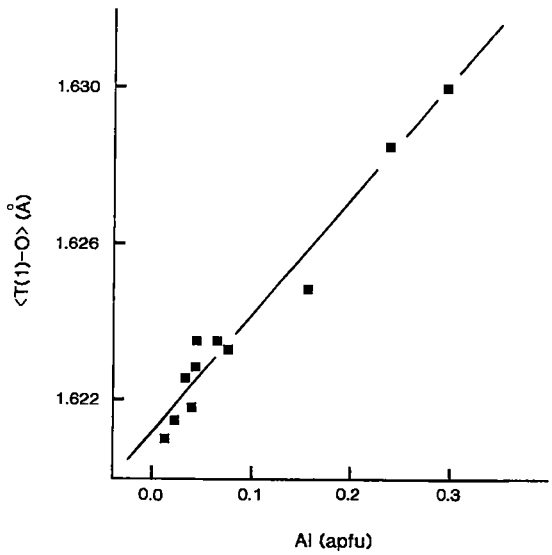

FIG. 1. Variation in <*T*(1)–O> as a function of [4]Al content in amphiboles from Coyote Peak.

contents of *M*(1) and *M*(3), and the F content of O(3). However, despite the significant variations in Fe^{2+} at *M*(1) and F at O(3), it is apparent from Figure 3a that Ti^{4+} and O^{2-} are major causes of the variation in *M*(1)–O(3) in these amphiboles, whereas they are not such a dominant influence on *M*(3)–O(3). Similarly, there is a contraction of the *M*(1)–*M*(1) distance and an increase in the *M*(1)–*M*(2) distance with increasing Ti^{4+} (Figs. 3c, d). These relations indicate that (1) $^{[6]}Ti^{4+}$ associated with O^{2-} at locally adjacent O(3) sites is strongly to completely ordered at the *M*(1) site, in line with substitution (1) described above, (2) the *M*(1)–*M*(2) distance correspondingly expands in response to the contracting *M*(1)–*M*(1) distance. This ordering of Ti^{4+} at *M*(1) and the concomitant contraction of the *M*(1)–*M*(1) distance with increasing Ti^{4+} is also in accord with the anomalously large and anisotropic displacement observed for the *M*(1) site in the more Ti-rich amphiboles of this study. We therefore assign all Ti^{4+} in excess of 0.13 *apfu* in amphiboles with OH + F < 2.0 *apfu* to the *M*(1) site; Ti up to 0.13 *apfu* is assigned to the *M*(2) site.

Total scattering at M(1), M(2) and M(3)

The site-scattering values were unconstrained in the refinement procedure, and the total scattering at the *M*(1), *M*(2) and *M*(3) sites represents the total number

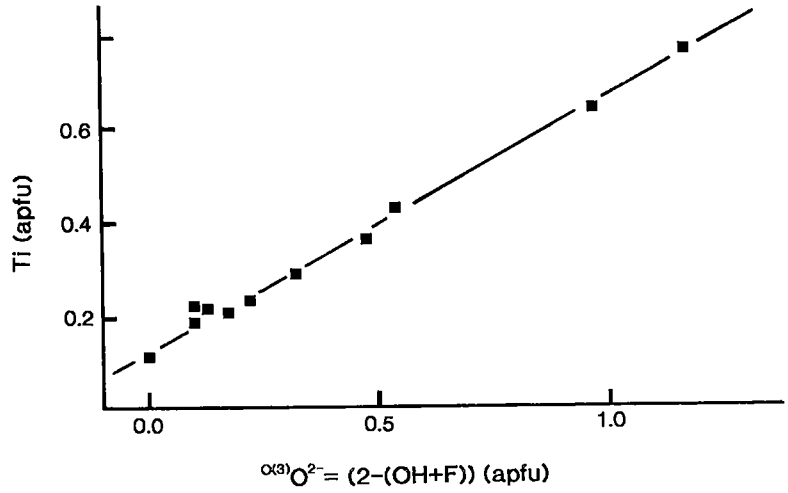

FIG. 2. Variation in Ti^{4+} as a function of the O^{2-} content of the O(3) site [2 – (OH + F)] in amphiboles from Coyote Peak. The line is a least-squares fit to the data points with OH + F ≠ 2.0: Ti = 0.13 + 0.52 [2 – (OH+ F)], R = 0.99.

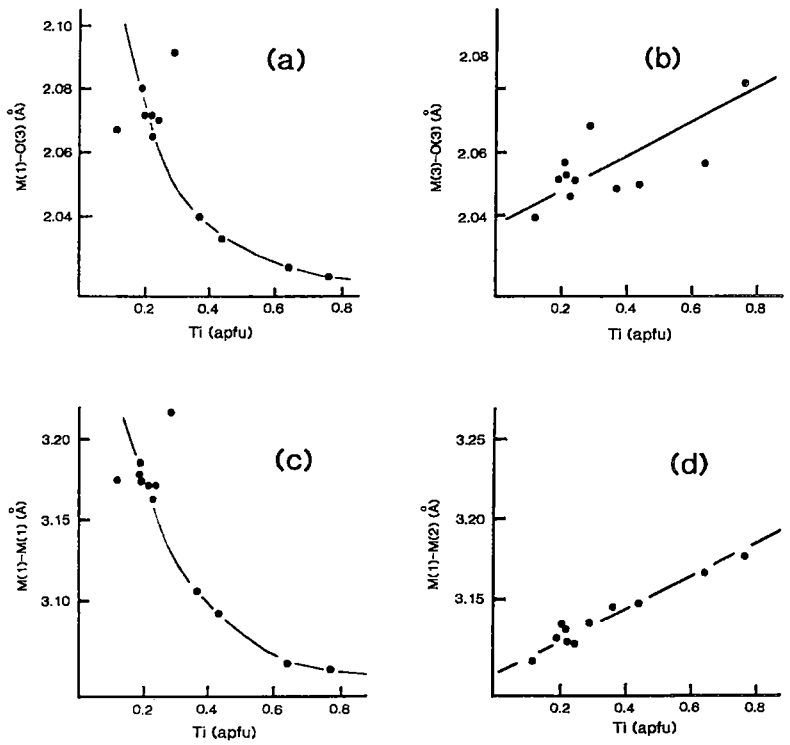

FIG. 3. Stereochemical variations about the O(3) site as a function of Ti^{4+} content in amphiboles from Coyote Peak: (a) M(1)–O(3), (b) M(3)–O(3), (c) M(1)–M(1), (d) M(1)–M(2).

of electrons (the mean atomic number when expressed per site) for the cations at these sites. The sum of the site scattering at the $M(1) + M(2) + M(3)$ sites can also be derived from the unit formulae calculated from the microprobe results, and comparison of these values gives a check on the consistency of both sets of results. A comparison is given in Table 4. The results agree closely, suggesting that there is no significant systematic error in either of the two sets of results.

Site populations at M(1), M(2) and M(3)

There are three sites with octahedral coordination, $M(1)$, $M(2)$ and $M(3)$. Because there are more than two scattering species per site, the total site-scattering cannot give a unique solution for the site populations (Hawthorne 1983b). However, for most chemically simple amphiboles, the microprobe results and the detailed stereochemical variations that accompany changes in site chemistry can be used in conjunction with the scattering results to give reliable site-populations (Ungaretti *et al.* 1983). The results of electron- and ion-microprobe analyses (Table 5) indicate that Mg, Fe, Ti, Mn and Li are *C*-group cations to be distributed over the $M(1)$, $M(2)$ and $M(3)$ sites. The minor Mn present is treated as equivalent to Fe: Fe* = Fe + Mn. The small amount of Li present is assigned to $M(3)$, following the results of Hawthorne *et al.* (1993). As Fe may occur in two valence states, the effective scattering species are thus Mg, Ti and Fe* (= $Fe^{2+} + Fe^{3+} + Mn^{2+}$) at these sites.

The site populations at $M(1)$, $M(2)$ and $M(3)$ were assigned as follows: $M(1)$: Mg and Fe^{2+} were assigned from the refined site-scattering values after subtracting the effect of Ti^{4+} assigned to $M(1)$ [$^{M(1)}Ti^{4+} = 1 - (OH + F)/2$]; $M(2)$: Ti^{4+} was assigned to $M(2)$ to a maximum of 0.13 *apfu*, and Mg and Fe^{2+} were assigned on the basis of the refined site-scattering values after subtracting the effect of Ti; the Fe^{3+} content of $M(2)$ was then calculated to obtain a neutral chemical formula; $M(3)$: Mg and Fe^{2+} were assigned from the refined site-scattering values after subtracting the effect of Li assigned to $M(3)$.

The M(4) site

The results of electron-microprobe analyses (Table 5) show that there is an insignificant amount of *C*-group cations at the $M(4)$ site, in accord with the absence of electron density at the $M(4')$ site in these amphiboles, except for 739 and 745, which show minor occupancy of the $M(4')$ site. Thus the refined site-scattering may be interpreted in terms of Ca and Na only. Table 4 compares the refined $M(4)$-site-scattering values with the effective scattering from the *B*-group cations in the unit formulae of Table 5; the highest difference (1.2 *e*) for 739 is due to the occurrence of *C*-group cations at the $M(4')$ site.

The A sites

Inspection of Table 5 shows that the *A*-site cavity is almost filled by Na and K, and the refined site-scattering values are in close agreement with the analyzed site-group contents (Table 4). In all amphiboles except 758, Na dominates over K at the *A* site.

The O(3) site

The O(3) site populations are one of the most interesting aspects of the current work, as they show explicitly that O^{2-} occurs in large quantities (0–1.17 *apfu*) at the O(3) site in these amphiboles (Tables 4, 6). The variation in OH, F and (implicitly) O^{2-} at O(3) in these amphiboles is shown in Figure 4. The squares denote amphiboles in which monovalent anions are dominant at the O(3) site. The star denotes an amphibole in which O^{2-} is dominant at O(3). It is apparent that the frequently made assumption that OH + F + Cl = 2 *apfu* in amphiboles does not hold for the Coyote Peak amphiboles. Furthermore, it is also apparent that the occurrence of O^{2-} at O(3) is not produced by *in situ* dehydrogenation accompanied by oxidation of Fe^{2+} to Fe^{3+}. In these amphiboles, there is a solid- solution series involving $^{M(1)}Ti^{4+} + 2^{O(3)}O^{2-} \rightarrow {}^{M(1)}(Mg,Fe^{2+}) + 2^{O(3)}OH$, and the amphiboles crystallized deficient in OH + F. Rearranging the regression equation of Figure 2 gives a predictive equation for the amount of O^{2-} at the O(3) site: $^{O(3)}O^{2-} = 1.89Ti - 0.25$. For the data used to construct the curve, the mean deviation from the "measured" value of O^{2-} is 0.03 *apfu*.

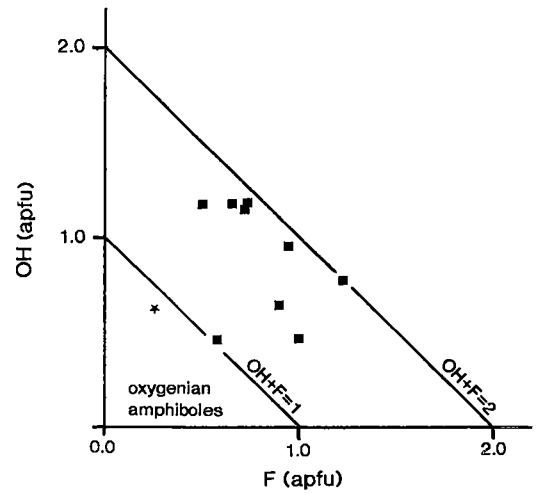

FIG. 4. Variation in OH as a function of F in amphiboles from Coyote Peak; star: an amphibole the end-member of which is anhydrous (*i.e.*, $^{O(3)}O^{2-} = 2.0$ *apfu*).

Unusual stereochemistry of the double chain of tetrahedra and the M(4) polyhedron

During a crystal-chemical study of a series of sodic to sodic–calcic to calcic amphiboles from eclogitized rocks of the Sesia – Lanzo Zone (Western Alps, Italy), Ungaretti *et al.* (1983) showed the existence of a structural gap related to the miscibility gap between sodic and sodic–calcic amphiboles. This gap is defined by a lack of observed values for the internal angles of the double chain of tetrahedra and for the conformation of the *M*(4) site. Of the nearly 800 crystal-structure refinements of amphiboles done at the CSCC in Pavia, none of the refined amphiboles fall into this structural gap. Figure 5a shows the plot of Ungaretti *et al.* (1983), modified by adding all additional available data and the refinements of the present work. Sodic amphiboles plot on the upper-right side of the gap, and the trend toward the lower left is related to the $^{[4]}$Al, $^{M(4)}$Ca and *A*-site occupancies. Samples of potassic-richterite fall to the left of sodic–calcic trend, whereas monoclinic Mg–Fe–Mn amphiboles fall to the right of the sodic trend.

The sodic–calcic amphiboles from the Coyote Peak diatreme continuously span the formerly prohibited zone, and the titanian oxygenian arfvedsonite 745 plots at the upper-right limit. Moreover, comparative analysis of the sodic–calcic amphiboles in our database showed that the present samples have the smallest values of *T*(1)–*T*(2)–*T*(1) and the largest values of *T*(2)–*T*(1)–*T*(1), confirming a deformation of the six-membered ring of tetrahedra due to stretching in the *b* direction. On the other hand, Figure 5b shows that the *A* + *M*(4) gap between sodic and sodic–calcic amphibole is not violated by these crystals.

Our crystal-chemical hypothesis was that the anomalous positions in Figure 5a were determined by the isovalent or heterovalent substitutions active at the octahedral sites, *i.e.*, $(Mg_{-1}Fe^{2+}$, $Al_{-1}Fe^{3+})$ and $[(Mg,Fe^{2+})_{-1}OH_{-2}TiO_2]$. Multiple-regression analysis of the changes in O(6)–O(5)–O(7) and [*M*(4)–O(5)] – [*M*(4)–O(6)] as a function of composition gave two excellent correlations: O(6)–O(5)–O(7) = 113.83(15) – 3.25(19) $^{M(4)}$Ca – 4.35(47) ^{T}Al + 1.08(11) O^{2-} (R = 0.994) and [*M*(4)–O(5)] – [*M*(4)–O(6)] = 0.414(6) – 0.091(5) $^{M(4)}$Ca – 0.095(11) ^{T}Al + 0.037(3) O^{2-} – 0.102(9) ^{A}K (R = 0.997). They show that the present samples span from the field of sodic–calcic amphiboles toward the upper-right due to dehydrogenation, and that the anomalous position of crystal 758 is due to its higher K content. The spanning of the geometrical gap is thus due to the different dimensional relations between the strip of octahedra and the double-chain of tetrahedra which, in turn, are a consequence of the extensive occurrence of O^{2-} at the O(3) site.

Problems with formulae of Ti-rich sodic amphiboles

In their work on the amphiboles from this locality, Czamanske & Atkin (1985) remarked on the fact that most of their amphibole formulae contain insufficient Si and Al to fill the tetrahedral sites. Ernst (1962) proposed that arfvedsonitic amphiboles formed at oxygen fugacities lower than those of the hematite–magnetite buffer are deficient in Si; he suggested that Fe^{3+} occurs in tetrahedral coordination in arfvedsonitic amphiboles formed under these conditions. As noted by Czamanske & Atkin (1985), this deficiency in (Si + Al) is typical of arfvedsonitic amphiboles occurring with titanian aegirine in peralkaline and undersaturated rocks (*e.g.*, Scott 1976, Rønsbo *et al.* 1977, Grapes *et al.* 1979, Nielsen 1979). Czamanske & Atkin (1985) chose to assign Ti^{4+} to the *T* sites, rather than Fe^{3+} as suggested by Ernst (1962). There has been no confirmed occurrence of $^{[4]}Fe^{3+}$ in amphiboles (Hawthorne 1983a), and the suggestion of Ernst (1962) is not considered viable. However, $^{[4]}$Ti has been confirmed in both natural and synthetic amphiboles. Oberti *et al.* (1992) have shown by X-ray site-scattering refinement that Ti can occur at the *T*(2) site in richterite from lamproitic rocks. Della Ventura *et al.* (1991, 1993) have shown that Ti occurs at the *T*(2) site in synthetic richterite and fluororichterite using Rietveld structure refinement. Thus the suggestion of Czamanske & Atkin (1985) that Ti^{4+} is a *T*-group cation in amphiboles from Coyote Peak seems reasonable, as these amphiboles are dominantly richterite or related species.

The current work on the Coyote Peak amphiboles shows that there is no tetrahedrally coordinated Ti in these amphiboles. So why did the previous work show a deficiency of (Si + Al)? An unusual feature of these amphiboles is that they contain significant O^{2-} at the O(3) site, *i.e.*, the amphiboles are deficient in monovalent anions relative to the usual assumption that (OH + F + Cl) = 2.0 *apfu*. This feature significantly affects the calculation of the unit formulae if the monovalent anions (specifically OH) are not determined. In order to examine the effect of this feature in the present case, we have calculated the unit formulae according to the method usually used for electron-microprobe data: the anion content is 24 *apfu* with OH + F + Cl = 2.0 *apfu* (*i.e*, a 23-oxygen normalization scheme), with the Fe^{3+} content calculated according to the method of Papike *et al.* (1974); values are given in Table 7 for those amphiboles for which OH + F << 2.0 *apfu*. Certain deviations from the usual distribution of cations in the amphibole structure are immediately apparent: (1) Si + Al < 8.0 *apfu*. The range of Si + Al in Table 7 is 7.95–7.82 *apfu*, and tends to decrease with decreasing OH + F. This behavior was also observed by Czamanske &

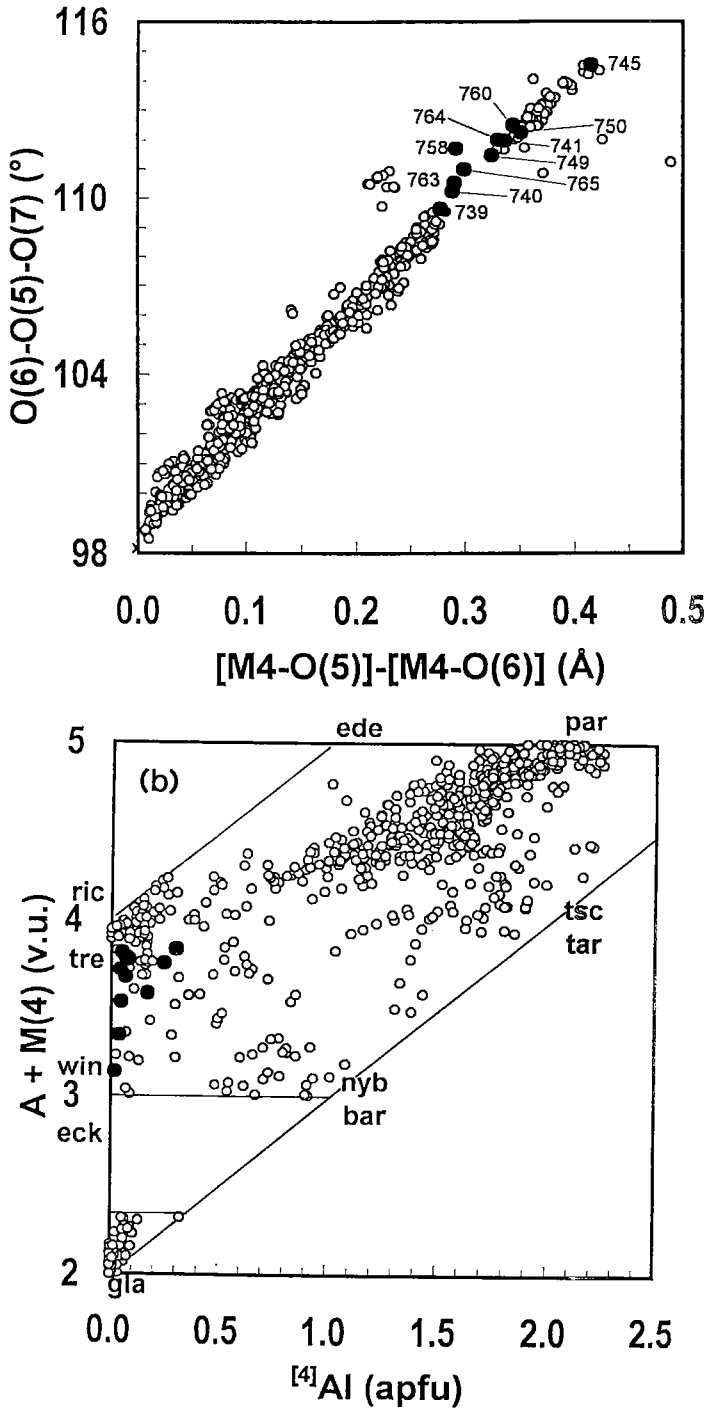

FIG. 5. (a) Variation in O(5)–O(6)–O(7) as a function of the difference betwen $M(4)$–O(5) and $M(4)$–O(6) in calcic, sodic–calcic and sodic amphiboles (after Ungaretti *et al.* 1983); the unshaded circles are data for ~800 refined amphiboles, the shaded circles are the amphiboles refined in this study. (b) Variation in charge at the $A + M(4)$ sites as a function of the amount of $^{[4]}$Al in calcic, sodic–calcic and sodic amphiboles (after Ungaretti *et al.* 1983); the legend is as in Figure 5a; ede: edenite; par: pargasite; ric: richterite; tre: tremolite; win: winchite; eck: eckermannite; gla: glaucophane; tsc: tschermakite; tar: taramite; nyb: nyböite; bar: barroisite.

Atkin (1985), who assigned Ti^{4+} to the *T*- group cations to bring the sum (Si + Al + Ti) up to the ideal value of 8 *apfu*. It is apparent from comparison of Tables 5 and 7 that unit formulae with Si + Al < 8 *apfu* are indicative of an inappropriate method of normalization (in this case assuming OH + F = 2 *apfu* when OH + F << 2 *apfu*). (2) The sum of the *C*-group cations is less than the minimum value of 5 *apfu*, whereas the ΣC values of Table 5 cluster around 5 *apfu*. Although the magnitudes of the deviations from 5 *apfu* in Table 7 are small (and any single example could be ascribed to error in the analysis), the fact that all values are systematically low indicates that this feature is also the result of inappropriate renormalization. In this regard, the data of Czamanske & Atkin (1985) also show low *C*-cation sums for Ti-rich (and hence OH + F poor) compositions. Also note that the Fe^{3+} contents (Table 7) are inferred to be zero. The results of the present work show that these amphiboles do, in fact, contain significant Fe^{3+} (Table 5). If the actual values of Fe^{3+}/Fe^{2+} are used in the same calculation used to produce the data of Table 7, the *T*- and *C*-cation sums become even smaller than those shown in Table 7.

From this discussion, we may identify certain compositional features in sodic–calcic and sodic amphiboles that indicate OH + F < 2 *apfu*: (1) the amphibole should be rich in Ti^{4+}; (2) the sum of the *T*-group cations is less than 8 *apfu*; (3) the sum of the *C*-group cations is less than 5 *apfu*.

TABLE 7. UNIT FORMULAE FOR COYOTE PEAK AMPHIBOLES [WITH ANALYZED (OH + F) < 2.0 *apfu*] CALCULATED WITH OH + F = 2.0 *apfu* AND Fe^{3+} ESTIMATED AFTER THE METHOD OF PAPIKE *et al.* (1974)

	741	749	750	745
Si	7.900	7.813	7.783	7.874
Al	0.044	0.065	0.040	0.016
ΣT	7.944	7.878	7.823	7.890
Al	–	–	–	–
Fe^{3+}	–	–	–	–
Fe^{2+}	1.369	1.539	2.100	2.815
Mn	0.017	0.032	0.041	0.019
Ti	0.358	0.433	0.630	0.746
Mg	3.206	2.965	2.146	1.284
Li	0.006	0.006	0.012	0.103
ΣC	4.956	4.975	4.929	4.967
Ca	0.720	0.844	0.751	0.145
Na	1.280	1.156	1.249	1.855
ΣB	2.000	2.000	2.000	2.000
Na	0.627	0.628	0.609	0.702
K	0.298	0.274	0.282	0.289
ΣA	0.925	0.902	0.891	0.991

It is interesting to compare the current results with those found by Hawthorne *et al.* (1993) for sodic amphiboles containing significant Li. In this case, omission of Li from the composition leads to formulae with (1) the sum of the *T*-group cations greater than 8 *apfu*; (2) the sum of the *C*-group cations is less than 5 *apfu*; (3) the sum of the *A*-group cations is commonly greater than 1 *apfu*. Comparison with the criteria listed above for (OH + F)-deficient amphiboles suggests that we can differentiate between these two compositional characteristics simply from the different patterns of cation sums in the unit formula.

Conclusions

(1) Electron microprobe and SIMS analysis of amphiboles from lithic-wacke inclusions in the Coyote Peak diatreme show that these amphiboles contain OH + F + Cl contents in the range $2.0 \leq OH + F + Cl \leq 0.84$ *apfu*. Hence these amphiboles have significant occupancy of the O(3) site by O^{2-}.

(2) The Ti content of the amphibole is linearly correlated with the O^{2-} content of the O(3) site ($R = 0.99$) according to the equation $Ti = 0.13 + 0.52 \times O^{2-}$.

(3) The above equation indicates that, in these amphiboles, Ti in excess of 0.13 *apfu* enters the structure according to the substitution $Ti + 2\ O^{2-} \rightarrow (Mg,Fe^{2+}) + 2\ OH$.

(4) The *M*(1)–O(3) and *M*(1)–*M*(1) distances decrease strongly as the Ti content of the amphibole increases, indicating that Ti in excess of 0.13 *apfu* occurs at the *M*(1) site.

(5) Consideration of the relation in (3), together with the <*M*(2)–O> and <*M*(3)–O> distances, indicates that up to 0.13 *apfu* Ti occurs at the *M*(2) site in these amphiboles.

(6) In the absence of direct determination of the H content of amphiboles, high Ti and Si + Al << 8.0 *apfu* are indicative of the presence of O^{2-} at the O(3) site (*i.e.*, OH = F + Cl << 2.0 *apfu*).

(7) The presence of O^{2-} at the O(3) site in these amphiboles induces a range of values of the O(5)–O(6)–O(7) angle, and a difference between the *M*(4)–O(5) and *M*(4)–O(6) bond lengths not found in normal [O(3) = OH,F] amphiboles.

Acknowledgements

We thank Giancarlo Della Ventura and an anonymous reviewer for their comments on this manuscript. FCH was supported by Natural Sciences and Engineering Research Council of Canada.

References

Cannillo, E., Hawthorne, F.C., Oberti, R. & Ungaretti, L. (1988): Anomalie nella composizione cristallochimica della porzione ottaedrica degli anfiboli. *Convegno Promaverile, Soc. Ital. Mineral. Petrogr., Abstr.*, 55.

CHARLES, R.W. (1977): The phase equilibria of intermediate compositions on the pseudobinary $Na_2CaMg_5Si_8O_{22}(OH)_2$ – $Na_2CaFe_5Si_8O_{22}(OH)_2$. *Am. J. Sci.* **277**, 594-625.

CZAMANSKE, G.K. & ATKIN, S.A. (1985): Metasomatism, titanian acmite, and alkali amphiboles in lithic-wacke inclusions within the Coyote Peak diatreme, Humboldt County, California. *Am. Mineral.* **70**, 499-516.

_____ & DILLET, B. (1988): Alkali amphibole, tetrasilicic mica, and sodic pyroxene in peralkaline siliceous rocks, Questa Caldera, New Mexico. *Am. J. Sci.* **288A**, 358-392.

DELLA VENTURA, G., ROBERT, J.-L. & BÉNY, J.-M. (1991): Tetrahedrally coordinated Ti^{4+} in synthetic Ti-rich potassic richterite: evidence fom XRD, FTIR and Raman studies. *Am. Mineral.* **76**, 1134-1140.

_____, _____, _____, RAUDSEPP, M. & HAWTHORNE, F.C. (1993): The OH–F substitution in Ti-rich potassium-richterite: Rietveld structure refinement and FTIR and micro-Raman spectroscopic studies of synthetic amphiboles in the system K_2O–Na_2O–CaO–MgO–SiO_2–TiO_2–H_2O–HF. *Am. Mineral.* **78**, 980-987.

ERNST, W.G. (1962): Synthesis, stability relations, and occurrence of riebeckite and riebeckite – arfvedsonite solid solutions. *J. Geol.* **70**, 689-736.

GRAPES, R., YAGI, K. & OKUMURA, K. (1979): Aenigmatite, sodic pyroxene, arfvedsonite and associated minerals in syenites from Morotu, Sakhalin. *Contrib. Mineral. Petrol.* **69**, 97-103.

HAWTHORNE, F.C. (1983a): The crystal chemistry of the amphiboles. *Can. Mineral.* **21**, 173-480.

_____ (1983b): Quantitative characterization of site-occupancies in minerals. *Am. Mineral.* **68**, 287-306.

_____, UNGARETTI, L., OBERTI, R., BOTTAZZI, P. & CZAMANSKE, G. (1993): Li: an important component in igneous alkali amphiboles. *Am. Mineral.* **78**, 733-745.

KITAMURA, M., TOKONAMI, M. & MORIMOTO, N. (1975): Distribution of titanium atoms in oxy-kaersutite. *Contrib. Mineral. Petrol.* **51**, 167-172.

LEAKE, B.E., WOOLLEY, A.R., ARPS, C.E.S, BIRCH, W.D., GILBERT, M.C., GRICE, J.D., HAWTHORNE, F.C., KATO, A., KISCH, H.J., KRIVOVICHEV, V.G., LINTHOUT, K., LAIRD, J., MANDARINO, J.A., MARESCH, W.V., NICKEL, E.H., ROCK, N.M.S., SCHUMACHER, J.C., SMITH, D.C., STEPHENSON, N.C.N., UNGARETTI, L., WHITTAKER, E.J.W. & YOUSHI, G. (1997): Nomenclature of amphiboles: report of the Subcommittee on Amphiboles of the International Mineralogical Association, Commission on New Minerals and Mineral Names. *Can. Mineral.* **35**, 219-246.

MORGAN, J.W., CZAMANSKE, G.K. & WANDLESS, G.A. (1985): Origin and evolution of the alkalic ultramafic rocks in the Coyote Peak diatreme, Humboldt County, California. *Geochim. Cosmochim. Acta* **49**, 749-759.

NIELSEN, T.F.D. (1979): The occurrence and formation of Ti-aegirines in peralkaline syenites. *Contrib. Mineral. Petrol.* **69**, 235-244.

OBERTI, R., HAWTHORNE, F.C., UNGARETTI, L. & CANNILLO, E. (1995b): $^{[6]}$Al disorder in amphiboles from mantle peridotites. *Can. Mineral.* **33**, 867-878.

_____, UNGARETTI, L., CANNILLO, E. & HAWTHORNE, F.C. (1992): The behaviour of Ti in amphiboles. I. Four- and six-coordinate Ti in richterite. *Eur. J. Mineral.* **4**, 425-439.

_____, _____, _____, _____ & MEMMI, I. (1995a): Temperature-dependent Al order – disorder in the tetrahedral double-chain of *C2/m* amphiboles. *Eur. J. Mineral.* **7**, 1049-1063.

OTTEN, M.T. & BUSECK, P.R. (1987): The oxidation state of Ti in hornblende and biotite determined by electron energy-loss spectroscopy with inferences regarding the Ti substitution. *Phys. Chem. Minerals* **14**, 45-51.

OTTOLINI, L., BOTTAZZI, P. & VANNUCCI, R. (1993): Quantification of lithium, beryllium and boron in silicates by secondary ion mass spectrometry using conventional energy filtering. *Anal. Chem.* **65**, 1960-1968.

_____, _____, ZANETTI, A. & VANNUCCI, R. (1995): Determination of hydrogen in silicates by secondary ion mass spectrometry. *Analyst* **120**, 1309-1313.

PAPIKE, J.J., CAMERON, K.L. & BALDWIN, K. (1974): Amphiboles and pyroxenes: characterization of other than quadrilateral components and estimates of ferric iron from microprobe data. *Geol. Soc. Am., Abstr. Program* **6**, 1053-1054.

PECHAR, F., FUESS, H. & JOSWIG, W. (1989): Refinement of the crystal structure of kaersutite (Vlčí Hora, Bohemia) from neutron diffraction. *Neues Jahrb. Mineral. Monatsh.*, 137-143.

RØNSBO, J.G., PEDERSEN, A.K. & ENGELL, J. (1977): Titan-aegirine from early Tertiary ash layers in northern Denmark. *Lithos* **10**, 193-204.

SCOTT, P.W. (1976): Crystallization trends of pyroxenes from the alkaline volcanic rocks of Tenerife, Canary Islands. *Mineral. Mag.* **40**, 805-816.

SHANNON, R.D. (1976): Revised effective ionic radii and systematic studies of interatomic distances in halides and chalcogenides. *Acta Crystallogr.* **A32**, 751-767.

UNGARETTI, L., LOMBARDO, B., DOMENEGHETTI, C. & ROSSI, G. (1983): Crystal-chemical evolution of amphiboles from eclogitized rocks of the Sesia – Lanzo Zone, Italian Western Alps. *Bull. Minéral.* **106**, 645-672.

WAYCHUNAS, G.A. (1987): Synchrotron radiation XANES spectroscopy of Ti in minerals: effects of Ti bonding distances, Ti valence and site geometry on absorption edge structure. *Am. Mineral.* **72**, 89-101.

Received October 27, 1997, revised manuscript accepted August 18, 1998.